CrossMark

J. Plasma Physics (2015), *vol.* 81, 905810323 © Cambridge University Press 2015
doi:10.1017/S0022377815000264

Non-axisymmetric local magnetostatic equilibrium

J. Candy† and E. A. Belli

General Atomics, P.O. Box 85608, San Diego, CA 92186-5608, USA

(Received 5 November 2014; revised 18 February 2015; accepted 23 February 2015; first published online 24 March 2015)

In this work we outline an approach to the problem of local equilibrium in non-axisymmetric configurations that adheres closely to Miller's original method for axisymmetric plasmas (Miller et al. 1998 *Phys. Plasmas* **5**, 973). Importantly, this method is novel in that it allows not only specification of 3D shape, but also explicit specification of the **shear** in the 3D shape. A spectrally-accurate method for solution of the resulting nonlinear partial differential equations is also developed. We verify the correctness of the spectral method, in the axisymmetric limit, through comparisons with an independent numerical solution. Some analytic results for the two-dimensional case are given, and the connection to Boozer coordinates is clarified.

1. Introduction

The local equilibrium method (Mercier and Luc 1974; Greene and Chance 1981; Bishop et al. 1984) is a powerful tool for providing metric coefficients required to evaluate the differential operators that appear in axisymmetric neoclassical, gyrokinetic, and MHD ballooning stability calculations. This approach ensures consistency with the equations of magnetostatic equilibrium (i.e. the Grad-Shafranov equation in the axisymmetric case). The approach suggested by Miller et al. (1998) is particularly useful insofar as one can specify not only the shape of the flux surface, but also the rates of change of the shape (for example, the Shafranov shift dR_0/dr, or the rate of change of elongation, $d\kappa/dr$) which are required for the solution of the gyrokinetic equations, for instance. Because the plasma behavior is known to have a strong dependence on these shape gradients, it is natural to construct a local equilibrium method for which they are independently adjustable. This was a strong motivation for Miller's method in 2D, and the present paper therefore clarifies how to apply the same approach in 3D. Although Miller's original formulation used nine parameters to characterize the equilibrium, this has been generalized to an arbitrary number of shape parameters to achieve any desired accuracy (Candy et al. 2009). Unlike a global equilibrium solver, the Miller approach allows for fast, systematic shaping studies on plasma transport and stability.

An analytical approach to the generalization of the local equilibrium method to three-dimensional configurations was described some time ago by Hegna (2000). The approach is elegant and maintains a strong connection to the underlying differential geometry. However, how to adapt the magnetic differential equations derived in that work to suit a Miller-type workflow is not discussed. Methods for numerical solution are also not discussed. The goal of the present work is to describe an alternative

† Email address for correspondence: candy@fusion.gat.com

https://doi.org/10.1017/S0022377815000264 Published online by Cambridge University Press

approach for the 3D problem that generalizes Miller's original one, and to develop a spectral method for solution of the resulting nonlinear partial differential equations. The resulting formalism should be suitable for neoclassical (Hirshman et al. 1986; van Rij and Hirshman 1989; Landreman et al. 2014), gyrokinetic (Waltz and Miller 1999; Xanthopoulos et al. 2007; Baumgaertel et al. 2011), and MHD ballooning (Bird and Hegna 2013) calculations in non-axisymmetric geometry.

The distinction between the present approach and that in Hegna (2000) is discussed by Boozer (2002). According to Boozer's characterization of the problem, in addition to the shape, there is a function $f_s(\bar{\theta}, \bar{\varphi})$ that must be specified. In the present work, that choice is $f_s(\bar{\theta}, \bar{\varphi}) = J_s(\bar{\theta}, \bar{\varphi})$, where J_s is a suitably normalized Jacobian. In Hegna's work, the choice is $f_s(\bar{\theta}, \bar{\varphi}) = \bar{\theta} - \theta$, where $\bar{\theta}$ is an arbitrary poloidal angle (the parametric angle in this work) and θ is the magnetic poloidal angle (the straight fieldline angle in this work).

The outline of the paper is as follows. In Sec. 2, we derive the general form of the equations for magnetostatic equilibrium. In Sec. 3, the Mercier–Luc expansion technique is generalized to non-axisymmetric flux-surface shape. The zeroth and first-order equations describing local equilibria are derived in Secs 4 and 5, respectively. And finally, in Sec. 6, we show how to write selected differential operators in terms of computed quantities.

2. Equations of magnetostatic equilibrium

2.1. *Magnetic field representation and tensor identities*

We concentrate on regions of the plasma where good magnetic surfaces exist, in which case the magnetic field can be written as

$$\boldsymbol{B} = \nabla z^1 \times \nabla(z^2 - \iota z^3) = \frac{1}{\sqrt{g}}\left(\frac{\partial \boldsymbol{x}}{\partial z^3} + \iota \frac{\partial \boldsymbol{x}}{\partial z^2}\right), \tag{2.1}$$

where $(z^1, z^2, z^3) \doteq (\chi, \theta, \varphi)$ are non-orthogonal toroidal coordinates with Jacobian

$$\sqrt{g} = \frac{\partial \boldsymbol{x}}{\partial z^1} \cdot \frac{\partial \boldsymbol{x}}{\partial z^2} \times \frac{\partial \boldsymbol{x}}{\partial z^3} = \frac{1}{\nabla z^1 \cdot \nabla z^2 \times \nabla z^3}. \tag{2.2}$$

In this representation, χ is the toroidal flux over 2π, whereas θ and φ are straight fieldline angles in the poloidal and toroidal directions. The rotation transform is given by $\iota = 1/q = d\chi/d\psi$, where q is the safety factor and ψ is the poloidal flux over 2π. Here, we note the transformation relations between the reciprocal bases

$$\nabla z^j = \sum_i g^{ij} \frac{\partial \boldsymbol{x}}{\partial z^i} \quad \leftrightarrow \quad \frac{\partial \boldsymbol{x}}{\partial z^j} = \sum_i g_{ij} \nabla z^i, \tag{2.3}$$

where ∇z^i and $\partial \boldsymbol{x}/\partial z^i$ are the contravariant and covariant vectors, respectively. In addition, we note the relation

$$\frac{\partial \boldsymbol{x}}{\partial z^i} = \sqrt{g}\, \nabla z^j \times \nabla z^k \quad \text{with} \quad \{ijk\} = \{123\}, \{231\}, \{312\}, \tag{2.4}$$

which implies the important orthogonality relation

$$\nabla z^i \cdot \frac{\partial \boldsymbol{x}}{\partial z^j} = \sum_k g^{ki} g_{kj} = \delta^i_j. \tag{2.5}$$

https://doi.org/10.1017/S0022377815000264 Published online by Cambridge University Press

Finally, the elements of the covariant and contravariant metric tensors are as follows:

$$g_{ij} \doteq \frac{\partial \boldsymbol{x}}{\partial z^i} \cdot \frac{\partial \boldsymbol{x}}{\partial z^j} \quad \text{and} \quad g^{ij} \doteq \nabla z^i \cdot \nabla z^j. \tag{2.6}$$

In what follows we will express all results in terms of the g_{ij}. In Appendix A, we outline the connection between the present coordinates and Boozer coordinates.

2.2. *Non-orthogonal, non-axisymmetric equilibrium formulation*

Momentum balance together with Ampère's law determine the basic equations of non-rotating magnetostatic equilibrium

$$\boldsymbol{J} \times \boldsymbol{B} = c \nabla p, \tag{2.7}$$

$$\nabla \times \boldsymbol{B} = \frac{4\pi}{c} \boldsymbol{J}. \tag{2.8}$$

Eliminating the current yields a single equation for the equilibrium

$$\frac{1}{4\pi} \boldsymbol{B} \cdot \nabla \boldsymbol{B} = \nabla \left(p + \frac{B^2}{8\pi} \right). \tag{2.9}$$

The orthogonality condition, (2.5), suggests that we take the projections along covariant bases:

$$(\boldsymbol{B} \cdot \nabla \boldsymbol{B}) \cdot \frac{\partial \boldsymbol{x}}{\partial z^i} = B \frac{\partial B}{\partial z^i} + 4\pi \frac{\partial p}{\partial z^i}, \tag{2.10}$$

yielding three scalar conditions for equilibrium. First, we note that the left-hand side of (2.10) is expressed naturally in terms of Christoffel symbols of the first kind

$$(\boldsymbol{B} \cdot \nabla \boldsymbol{B}) \cdot \frac{\partial \boldsymbol{x}}{\partial z^i} = \frac{1}{g} \left([33, i] + 2\iota [23, i] + \iota^2 [22, i] \right) + \frac{g_{i3} + \iota g_{i2}}{\sqrt{g}} \partial_\ell \left(\frac{1}{\sqrt{g}} \right), \tag{2.11}$$

where

$$[ij, k] \doteq \frac{1}{2} \left(\frac{\partial g_{ik}}{\partial z^j} + \frac{\partial g_{jk}}{\partial z^i} - \frac{\partial g_{ij}}{\partial z^k} \right), \tag{2.12}$$

and $\partial_\ell = \partial/\partial z_3 + \iota \partial/\partial z_2$. From this result is it easy to show

$$\partial_\ell \left(\frac{g_{i3} + \iota g_{i2}}{\sqrt{g}} \right) - \frac{\partial}{\partial z^i} \left(\frac{g_{33} + 2\iota g_{23} + \iota^2 g_{22}}{\sqrt{g}} \right) + \iota' \left(\frac{g_{23} + \iota g_{22}}{\sqrt{g}} \right) \delta_i^1 = 4\pi \sqrt{g} p' \delta_i^1, \tag{2.13}$$

where a prime denotes a derivative with respect to z^1.

2.3. *Radial current*

Setting $i = 2, 3$ gives the same result, namely, the condition for *zero radial current*

$$\frac{\partial}{\partial z^2} \left(\frac{g_{33} + \iota g_{23}}{\sqrt{g}} \right) = \frac{\partial}{\partial z^3} \left(\frac{g_{23} + \iota g_{22}}{\sqrt{g}} \right). \tag{2.14}$$

2.4. *Force balance*

Setting $i = 1$ gives the condition for *radial force balance*

$$\partial_\ell \left(\frac{g_{13} + \iota g_{12}}{\sqrt{g}} \right) - \frac{\partial}{\partial z^1} \left(\frac{g_{33} + 2\iota g_{23} + \iota^2 g_{22}}{\sqrt{g}} \right) + i' \left(\frac{g_{23} + \iota g_{22}}{\sqrt{g}} \right) = 4\pi \sqrt{g} p'. \tag{2.15}$$

Together, (2.14) and (2.15) are the scalar conditions for three-dimensional magnetostatic equilibrium.

https://doi.org/10.1017/S0022377815000264 Published online by Cambridge University Press

2.5. *Metric elements*

Writing the position vector as

$$\boldsymbol{x} = R\sin\varphi\,\boldsymbol{e}_x + R\cos\varphi\,\boldsymbol{e}_y + Z\boldsymbol{e}_z, \tag{2.16}$$

the metric elements become

$$g_{33} = g_{\varphi\varphi} = \frac{\partial \boldsymbol{x}}{\partial \varphi}\cdot\frac{\partial \boldsymbol{x}}{\partial \varphi} = R^2 + \left(\frac{\partial R}{\partial \varphi}\right)^2 + \left(\frac{\partial Z}{\partial \varphi}\right)^2, \tag{2.17}$$

$$g_{22} = g_{\theta\theta} = \frac{\partial \boldsymbol{x}}{\partial \theta}\cdot\frac{\partial \boldsymbol{x}}{\partial \theta} = \left(\frac{\partial R}{\partial \theta}\right)^2 + \left(\frac{\partial Z}{\partial \theta}\right)^2, \tag{2.18}$$

$$g_{23} = g_{\theta\varphi} = \frac{\partial \boldsymbol{x}}{\partial \theta}\cdot\frac{\partial \boldsymbol{x}}{\partial \varphi} = \frac{\partial R}{\partial \theta}\frac{\partial R}{\partial \varphi} + \frac{\partial Z}{\partial \theta}\frac{\partial Z}{\partial \varphi}, \tag{2.19}$$

$$g_{13} = g_{\chi\varphi} = \frac{\partial \boldsymbol{x}}{\partial \chi}\cdot\frac{\partial \boldsymbol{x}}{\partial \varphi} = \frac{\partial R}{\partial \chi}\frac{\partial R}{\partial \varphi} + \frac{\partial Z}{\partial \chi}\frac{\partial Z}{\partial \varphi}, \tag{2.20}$$

$$g_{12} = g_{\chi\theta} = \frac{\partial \boldsymbol{x}}{\partial \chi}\cdot\frac{\partial \boldsymbol{x}}{\partial \theta} = \frac{\partial R}{\partial \chi}\frac{\partial R}{\partial \theta} + \frac{\partial Z}{\partial \chi}\frac{\partial Z}{\partial \theta}. \tag{2.21}$$

The Jacobian takes the form

$$\sqrt{g} = \frac{\partial \boldsymbol{x}}{\partial \chi}\cdot\frac{\partial \boldsymbol{x}}{\partial \theta}\times\frac{\partial \boldsymbol{x}}{\partial \varphi} = R\left(\frac{\partial R}{\partial \chi}\frac{\partial Z}{\partial \theta} - \frac{\partial R}{\partial \theta}\frac{\partial Z}{\partial \chi}\right). \tag{2.22}$$

We can also associate poloidal and toroidal fields with the directions of the covariant bases; that is

$$\boldsymbol{B} = \boldsymbol{B}_p + \boldsymbol{B}_t, \tag{2.23}$$

where

$$\boldsymbol{B}_p = \frac{\iota}{\sqrt{g}}\frac{\partial \boldsymbol{x}}{\partial \theta} \longrightarrow B_p = \sqrt{\boldsymbol{B}_p\cdot\boldsymbol{B}_p} = \iota\frac{\sqrt{g_{\theta\theta}}}{\sqrt{g}}, \tag{2.24}$$

$$\boldsymbol{B}_t = \frac{1}{\sqrt{g}}\frac{\partial \boldsymbol{x}}{\partial \varphi} \longrightarrow B_t = \sqrt{\boldsymbol{B}_t\cdot\boldsymbol{B}_t} = \frac{\sqrt{g_{\varphi\varphi}}}{\sqrt{g}}, \tag{2.25}$$

and

$$B = \frac{1}{\sqrt{g}}\sqrt{g_{\varphi\varphi} + \iota^2 g_{\theta\theta} + 2\iota g_{\theta\varphi}}. \tag{2.26}$$

3. The local equilibrium perspective

Solving the equilibrium equations globally is a formidable task (Hirshman and Whitson 1983) that is fraught with theoretical difficulties related to rational surfaces. Rational surfaces are singularities of the ideal system. In reality, the plasma pressure is a kinetic quantity through which dissipative effects appear. This dissipation provides the physical means to regularize the system, but to include dissipation rigorously (through the Fokker–Planck collision operator) would require solving an intractable kinetic system. The local equilibrium approach here offers a useful alternative to a global solution as we can focus, for example, on a single irrational q for which the problem is non-singular.

3.1. *Axisymmetric formulation*

The Mercier–Luc (Mercier and Luc 1974) approach to axisymmetric local equilibrium requires the parametric specification of the flux surface via $R_s(\bar{\theta}_s)$ and $Z_s(\bar{\theta}_s)$, together

https://doi.org/10.1017/S0022377815000264 Published online by Cambridge University Press

with the poloidal field $B_{ps}(\bar{\theta}_s)$ on the surface. Here, $\bar{\theta}_s$ is a parametric angle that is *not* in general equal to the straight fieldline angle θ, and the subscript s refers to a reference surface. Miller et al. (1998) innovation to this approach was to use a radially continuous form for R and Z valid not only on the surface, but also in a neighborhood of the surface. In this way B_{ps} (together with R_s and Z_s) can be computed from R, Z and their derivatives. However, once B_{ps} is specified, the global forms for R, Z must be discarded and all non-local behavior subsequently determined by solution of the current and force balance equations. This approach allows one to not only to specify the shape, but also effects that depend on the derivative of the shape (Shafranov shift, elongation shear, etc).

3.2. *Non-axisymmetric formulation*

To generalize Miller's approach to non-axisymmetric systems, we first specify a parameterization of the flux surface $R_p(\bar{\theta}, \bar{\varphi}, \bar{r})$ and $Z_p(\bar{\theta}, \bar{\varphi}, \bar{r})$, where the subscript p means *parameterized*. These forms are taken to hold both on the reference surface as well as in the neighborhood of that surface. The explicit form of the parameterization is not important. Some models for the 2D case are discussed in Candy et al. (2009). This parameterization is then used to compute three surface functions R_s, Z_s and J_s, where

$$R_s(\bar{\theta}_s, \bar{\varphi}_s) = R_p(\bar{\theta}_s, \bar{\varphi}_s, \bar{r}_s), \tag{3.1}$$

$$Z_s(\bar{\theta}_s, \bar{\varphi}_s) = Z_p(\bar{\theta}_s, \bar{\varphi}_s, \bar{r}_s), \tag{3.2}$$

$$J_s(\bar{\theta}_s, \bar{\varphi}_s) = R_p \left(\frac{\partial R_p}{\partial \bar{r}} \frac{\partial Z_p}{\partial \bar{\theta}} - \frac{\partial R_p}{\partial \bar{\theta}} \frac{\partial Z_p}{\partial \bar{r}} \right) \Bigg|_{\boldsymbol{x}=\boldsymbol{x}_s}. \tag{3.3}$$

Above, $\boldsymbol{x} = \boldsymbol{x}_s$ implies that the derivatives should be taken with respect to the variables as indicated, and then the result evaluated on the flux-surface. In terms of the surface functions, we can write the Jacobian on the surface as

$$\sqrt{g_s} = \frac{J_s(\bar{\theta}_s, \bar{\varphi}_s)}{d\chi/dr} \frac{\partial \bar{\theta}_s}{\partial \theta_s}. \tag{3.4}$$

Note that this approach ensures that the surface Jacobian is consistent with radial dependence of the parameterization. This is in contrast to Hegna's treatment (Hegna 2000), for which the Jacobian is not determined by the surface parameterization. This feature is also discussed by Boozer (2002). Now, knowing the three surface functions, we *discard* the parameterization (R_p, Z_p). As explained in Sec. 4 of Miller et al. (1998), the parameterization for nearby surfaces is only a device to specify the single surface function J_s, and moreover, the description of nearby surfaces will not be exactly the same as (R_p, Z_p). That is why the latter parameterization must be discarded. Thus, the total information we will supply to specify a local equilibrium is in effect the same as in Miller et al. (1998); namely, (1) the shape (R_s, Z_s), (2) the Jacobian J_s and (3) the three numbers $dp/d\chi|_s$, ι_s and $d\iota/d\chi|_s$ where p and ι are the pressure and rotational transform.

In (3.4), $d\chi/dr \doteq r B_{\text{unit}}$, where B_{unit} is the effective magnetic field strength on the flux surface (Waltz and Miller 1999) and r is a suitably chosen length. In 2D, r is the half-width of the flux-surface at the elevation of the centroid (just a very general definition of the minor radius). In 3D, r can be defined as the toroidal average of the 2D definition, but different definitions are possible. In general, small alterations in the definition of r will give rise to small alterations in B_{unit}. In the absence of a global equilibrium, B_{unit} is a free parameter as explained in Candy (2009). The

https://doi.org/10.1017/S0022377815000264 Published online by Cambridge University Press

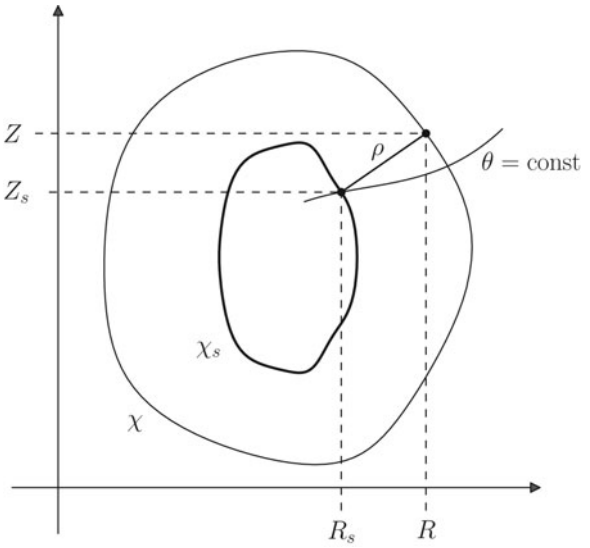


FIGURE 1. Illustration of coordinate system defined in (3.8) and (3.9) for a fixed toroidal angle φ_s. Whereas the reference flux surface, χ_s, has $\rho = 0$ everywhere on the surface, an adjacent flux surface, χ, is not a surface of constant ρ. Further, the segment labeled ρ, on which $\theta_s = \text{const}$, is not the same as the arc $\theta = \text{const}$.

parametric coordinates $(\bar{\theta}, \bar{\varphi}, \bar{r})$ are related to the straight fieldline coordinates via the transformation

$$\bar{r} = r, \tag{3.5}$$

$$\bar{\theta} = \bar{\theta}(r, \theta, \varphi), \tag{3.6}$$

$$\bar{\varphi} = \varphi. \tag{3.7}$$

We emphasize that the explicit form of the transformation is not yet known. Later, it will be determined by the condition of zero radial current. The strategy to obtain a local equilibrium solution will be to first represent R and Z both on the reference surface, and in the neighborhood of that surface, in $(\rho, \theta_s, \varphi_s)$ coordinates via

$$R(r, \theta, \varphi) = R_s + \rho \cos u(\theta_s, \varphi_s), \tag{3.8}$$

$$Z(r, \theta, \varphi) = Z_s + \rho \sin u(\theta_s, \varphi_s). \tag{3.9}$$

Above, $R_s = R_s(\bar{\theta}(r_s, \theta_s, \varphi_s), \varphi_s)$ and $Z_s = Z_s(\bar{\theta}(r_s, \theta_s, \varphi_s), \varphi_s)$. Because the transformation to the parametric angle is not yet known, in what follows we will work explicitly with θ_s as the independent variable. The relation between r (or equivalently, χ) and ρ is not known *a priori* and must be computed. An illustration of the coordinate system is shown in Fig. 1. In the equations above, u is the frame angle of the curve represented by the intersection of the reference flux surface and the toroidal plane $\varphi = \varphi_s$. Specifically,

$$\sin u = -\frac{1}{\ell_\theta}\frac{\partial R_s}{\partial \theta_s} \quad \text{and} \quad \cos u = \frac{1}{\ell_\theta}\frac{\partial Z_s}{\partial \theta_s}, \tag{3.10}$$

where

$$\ell_\theta^2 = \left(\frac{\partial R_s}{\partial \theta_s}\right)^2 + \left(\frac{\partial Z_s}{\partial \theta_s}\right)^2. \tag{3.11}$$

https://doi.org/10.1017/S0022377815000264 Published online by Cambridge University Press

We can also write

$$\frac{\partial u}{\partial \theta_s} = \frac{\ell_\theta}{r_\theta} \quad \text{and} \quad \frac{\partial u}{\partial \varphi_s} = \frac{\ell_\theta}{r_\varphi}, \tag{3.12}$$

where r_θ and r_φ are the poloidal and toroidal radii of curvature. We write the connection between the original (χ, θ, φ)-coordinates and the non-flux $(\rho, \theta_s, \varphi_s)$-coordinates via an expansion in the small parameter ρ

$$\chi = \chi_s + \rho\, \chi_1(\theta_s, \varphi_s) + \rho^2\, \chi_2(\theta_s, \varphi_s) + \cdots, \tag{3.13}$$

$$\theta = \theta_s + \rho\, \theta_1(\theta_s, \varphi_s) + \cdots, \tag{3.14}$$

$$\varphi = \varphi_s. \tag{3.15}$$

Derivatives can then be expressed in terms of the free functions χ_1, χ_2, and θ_1 according to

$$\frac{\partial}{\partial \chi} \sim \frac{1}{\chi_1}\left[1 + \rho\left(\frac{\partial \ln \chi_1}{\partial \theta_s} - \delta\chi\right)\right]\frac{\partial}{\partial \rho} - \delta\theta\left[1 - \rho\left(\delta\chi + \chi_1 \frac{\partial\, \delta\theta}{\partial \theta_s}\right)\right]\frac{\partial}{\partial \theta_s}, \tag{3.16}$$

$$\frac{\partial}{\partial \theta} \sim -\left(\rho\, \frac{\partial \ln \chi_1}{\partial \theta_s}\right)\frac{\partial}{\partial \rho} + \left(1 - \rho \chi_1 \frac{\partial\, \delta\theta}{\partial \theta_s}\right)\frac{\partial}{\partial \theta_s}, \tag{3.17}$$

$$\frac{\partial}{\partial \varphi} \sim -\left(\rho\, \frac{\partial \ln \chi_1}{\partial \varphi_s}\right)\frac{\partial}{\partial \rho} - \left(\rho\, \chi_1 \frac{\partial\, \delta\theta}{\partial \varphi_s}\right)\frac{\partial}{\partial \theta_s} + \frac{\partial}{\partial \varphi_s}, \tag{3.18}$$

where

$$\delta\theta \doteq \frac{\theta_1}{\chi_1} \quad \text{and} \quad \delta\chi \doteq \frac{2\chi_2}{\chi_1^2}. \tag{3.19}$$

Whereas determination of χ_1 is straightforward, we must solve a system of differential equations for $\delta\theta$ and $\delta\chi$. To illustrate the expansion procedure, we write

$$\sqrt{g} \sim \frac{\ell_\theta R_s}{\chi_1}\left[1 + \rho\left(\frac{1}{r_\theta} + \frac{\cos u}{R_s} - \delta\chi - \chi_1 \frac{\partial\, \delta\theta}{\partial \theta_s}\right)\right] + \mathcal{O}(\rho^2). \tag{3.20}$$

This implies that

$$\chi_1 = \frac{\ell_\theta R_s}{\sqrt{g_s}}, \tag{3.21}$$

where $\sqrt{g_s}$ is given by (3.4).

4. Zeroth-order equilibrium

4.1. *Nonlinear equation for the mapping*

In zeroth order, the condition for zero radial current becomes

$$\mathscr{C} = \frac{\partial}{\partial \theta}\left(\frac{N_0}{\sqrt{g_s}}\right) - \frac{\partial}{\partial \varphi}\left(\frac{M_0}{\sqrt{g_s}}\right) = 0, \tag{4.1}$$

where

$$M_0 = \iota_s \ell_\theta^2 + g_{\theta\varphi,s}, \tag{4.2}$$

$$N_0 = R_s^2 + \ell_\varphi^2 + \iota_s g_{\theta\varphi,s}, \tag{4.3}$$

$$\ell_\varphi^2 = \left(\frac{\partial R_s}{\partial \varphi_s}\right)^2 + \left(\frac{\partial Z_s}{\partial \varphi_s}\right)^2. \tag{4.4}$$

https://doi.org/10.1017/S0022377815000264 Published online by Cambridge University Press

In these expressions, $g_{\theta\varphi,s}$ is the metric element defined in Sec. 2.5 evaluated on the reference surface. The subtlety associated with (4.1) is that R_s, Z_s and J_s are explicit functions of an unknown mapping function $\bar{\theta}$. For this reason, it is necessary to evaluate the derivatives in the fieldline following coordinates using the chain rule

$$\frac{\partial}{\partial \theta_s} = \frac{\partial \bar{\theta}}{\partial \theta_s}\frac{\partial}{\partial \bar{\theta}}, \tag{4.5}$$

$$\frac{\partial}{\partial \varphi_s} = \frac{\partial \bar{\theta}}{\partial \varphi_s}\frac{\partial}{\partial \bar{\theta}} + \frac{\partial}{\partial \bar{\varphi}}. \tag{4.6}$$

Thus, (4.1) is a nonlinear partial differential equation for the coordinate transformation $\bar{\theta} = \bar{\theta}(\theta_s, \varphi_s)$.

4.2. *Numerical method for calculation of* $\bar{\theta}(\theta, \varphi)$

Equation (4.1) is a non-standard type of equation that is challenging to solve numerically. In what follows we outline a numerical method for solution. The foundation of the method is the expansion

$$\bar{\theta} = \theta + \sum_{m=0}^{N_\theta}\sum_{n=0}^{N_\varphi}\Big\{\sin(m\theta)\,[a_{mn}\cos(n\varphi) + b_{mn}\sin(n\varphi)] + \cos(m\theta)\,[c_{mn}\cos(n\varphi) + d_{mn}\sin(n\varphi)]\Big\}. \tag{4.7}$$

The conditions on the Fourier coefficients are

$$a_{mn} = 0 \quad \text{if } m = 0, \tag{4.8}$$

$$b_{mn} = 0 \quad \text{if } m = 0 \text{ or } n = 0, \tag{4.9}$$

$$c_{mn} = 0 \quad \text{if } m + n = 0, \tag{4.10}$$

$$d_{mn} = 0 \quad \text{if } n = 0. \tag{4.11}$$

The condition on c_{00} is arbitrary and sets an overall constant to zero. We can write this rather cumbersome expression more compactly as

$$\bar{\theta} = \theta + \sum_{p=0}^{N-1}\alpha_p \mathscr{F}_p(\theta, \varphi), \tag{4.12}$$

where p is the lumped Fourier index, $N = 1 + 4N_\theta N_\varphi + 2(N_\theta + N_\varphi)$, and $\mathscr{F}_p$ is defined in Table 1. By taking the residual to be orthogonal to the finite Fourier series, and using integration by parts to ensure all derivatives are carried out analytically, we can write the equations for the undetermined coefficients α_p as

$$\int_0^{2\pi} d\theta \int_0^{2\pi} d\varphi \left[\frac{\partial \mathscr{F}_p}{\partial \varphi}\left(\frac{M_0}{\sqrt{g_s}}\right) - \frac{\partial \mathscr{F}_p}{\partial \theta}\left(\frac{N_0}{\sqrt{g_s}}\right)\right] = 0. \tag{4.13}$$

Note that $p = 0$ is trivially satisfied, indicating that $c_{00} = \alpha_0$ is arbitrary. To evaluate the integrals we use numerical integration. Because the range of integration is over a periodic interval, equally-spaced nodes are optimal and give spectral accuracy. Specifically, we use the rule

$$\int_0^{2\pi} d\theta \int_0^{2\pi} d\varphi\, f(\theta, \varphi) \to \frac{1}{M_\theta M_\varphi}\sum_{i=0}^{M_\theta - 1}\sum_{j=0}^{M_\varphi - 1} f(\theta_i, \varphi_j), \tag{4.14}$$

https://doi.org/10.1017/S0022377815000264 Published online by Cambridge University Press

Coefficient	p	$\mathscr{F}_p(\theta, \varphi)$
c_{00}	0	1
a_{m0}	m	$\sin(m\theta)$
c_{m0}	$N_\theta + m$	$\cos(m\theta)$
c_{0n}	$2N_\theta + n$	$\cos(n\varphi)$
d_{0n}	$2N_\theta + N_\varphi + n$	$\sin(n\varphi)$
a_{mn}	$1 + \omega_{mn}$	$\sin(m\theta)\cos(n\varphi)$
b_{mn}	$2 + \omega_{mn}$	$\sin(m\theta)\sin(n\varphi)$
c_{mn}	$3 + \omega_{mn}$	$\cos(m\theta)\cos(n\varphi)$
d_{mn}	$4 + \omega_{mn}$	$\cos(m\theta)\sin(n\varphi)$

TABLE 1. Explicit description of 2D Fourier basis, where $\omega_{mn} \doteq 2(N_\theta + N_\varphi) + 4(n-1) + 4N_\varphi(m-1)$. Note that all entries assume $1 \leqslant m \leqslant N_\theta$ and $1 \leqslant n \leqslant N_\varphi$.

where $\theta_i = 2\pi i/M_\theta$, $\varphi_j = 2\pi j/M_\varphi$, $M_\theta = 2(N_\theta + 1)$ and $M_\varphi = 2(N_\varphi + 1)$. The result is a spectrally-accurate system of $N-1$ nonlinear algebraic equations for the coefficients $(\alpha_1, \ldots, \alpha_N)$. To solve the nonlinear system, we use the HYBRD1 routine from MINPACK (Moré et al. 1980).

4.3. *Example: an axisymmetric shifted circle*

It is useful to develop some intuition, and to contrast the differences between the present work and Hegna (2000), by examining the zero radial current condition for the simple case of an axisymmetric circular plasma. We begin with a non-local parameterization $\{R_p, Z_p\}$ (see Sec. 3.2) for a shifted circle

$$R_p(r, \bar{\theta}) = R_0(r) + r\cos\bar{\theta}, \tag{4.15}$$

$$Z_p(r, \bar{\theta}) = r\sin\bar{\theta}. \tag{4.16}$$

The implies the surface parameterization $\{R_s, Z_s, J_s\}$, where

$$R_s(\bar{\theta}_s) = R_{0s} + r_s\cos\bar{\theta}_s, \tag{4.17}$$

$$Z_s(\bar{\theta}_s) = r_s\sin\bar{\theta}_s, \tag{4.18}$$

$$J_s(\bar{\theta}_s) = r_s R_s\left(1 + \Delta_s\cos\bar{\theta}_s\right). \tag{4.19}$$

Above, we write the Shafranov shift on the surface as Δ_s, where $\Delta \doteq dR_0/dr$. Note the explicit appearance of Δ_s in the Jacobian J_s. In the axisymmetric case, (4.1) is solved via a trivial integration

$$\frac{\partial}{\partial\theta_s}\left(\frac{R_s^2}{\sqrt{g_s}}\right) = 0 \quad \rightarrow \quad \frac{R_s^2}{\sqrt{g_s}} = I_s, \tag{4.20}$$

where I_s is a constant of integration. Inserting J_s into the expression above yields a nonlinear, first-order ODE for the parametric angle $\bar{\theta}_s(\theta_s)$

$$\frac{R_{0s}}{r_s} + \cos\bar{\theta}_s = \frac{I_s}{d\chi/dr}\left(1 + \Delta_s\cos\bar{\theta}_s\right)\frac{\partial\bar{\theta}_s}{\partial\theta_s}. \tag{4.21}$$

This equation can be solved for arbitrary Δ_s. However, without the freedom to specify the parametric angle, there is no mechanism to explicitly set the Shafranov shift (or more generally, the gradient of the shape). For example, in the absence of a

https://doi.org/10.1017/S0022377815000264 Published online by Cambridge University Press

parametric angle, the surface parameterization would be

$$R_s(\theta_s) = R_{0s} + r_s \cos\theta_s, \tag{4.22}$$

$$Z_s(\theta_s) = r_s \sin\theta_s. \tag{4.23}$$

Attempting to use the previous Jacobian, J_s, would yield a current constraint

$$\frac{R_{0s}}{r_s} + \cos\theta_s = \frac{I_s}{d\chi/dr}\left(1 + \Delta_s \cos\theta_s\right), \tag{4.24}$$

for which a solution is possible only if $\Delta_s = r_s/R_{0s}$. Thus, without the use of a parametric angle, there does not appear to be a systematic way to control the gradient of the flux-surface shape. This provides the critical contrast between the present work and the treatment in Hegna (2000). In the latter case, the gradient of the shape is not defined in the parameterization, and (4.1) is viewed as a linear equation for $\sqrt{g_s}$. Conversely, in the present case, the gradient of the shape is defined by the parameterization, and this extra freedom makes (4.1) a nonlinear PDE for $\bar{\theta}_s$.

By considering the limit $\epsilon = r_s/R_{0s} \to 0$, and ordering $\Delta_s \sim \mathcal{O}(\epsilon)$, we can solve (4.21) to obtain

$$\frac{I_s}{d\chi/dr} \sim \frac{1}{\epsilon} + \frac{1}{2}\left(\epsilon + \Delta_s - \frac{{\Delta_s}^2}{\epsilon}\right) + \mathcal{O}(\epsilon^3), \tag{4.25}$$

$$\bar{\theta}_s \sim \theta_s + (\epsilon - \Delta_s)\sin\theta_s + \frac{1}{4}\left(\epsilon^2 - \epsilon\Delta_s - {\Delta_s}^2\right)\sin 2\theta_s + \mathcal{O}(\epsilon^3). \tag{4.26}$$

This formula can be used as a simple check on the accuracy of the numerical solution of (4.7), or to provide an initial guess for the rootfinder.

5. First-order equilibrium

5.1. *Linear equations for current and force balance*

After lengthy algebra, we find coupled linear differential equations for the functions $\delta\theta$ and $\delta\chi$

$$\begin{bmatrix} A_{11} & A_{12} \\ A_{21} & A_{22} \end{bmatrix} \begin{bmatrix} \delta\theta \\ \delta\chi \end{bmatrix} = \begin{bmatrix} S_1 \\ S_2 \end{bmatrix}, \tag{5.1}$$

where $\delta\theta$ and $\delta\chi$ are defined in (3.19), and

$$A_{11} f = \frac{M_0}{\sqrt{g_s}}\frac{\partial f}{\partial \varphi_s} - \frac{N_0}{\sqrt{g_s}}\frac{\partial f}{\partial \theta_s}, \tag{5.2}$$

$$A_{12} f = -\frac{N_0 + \iota_s M_0}{\sqrt{g_s}} f, \tag{5.3}$$

$$A_{21} f = \frac{\partial}{\partial \theta_s}\left(\frac{-2M_0 + \iota_s \ell_\theta^2}{\sqrt{g_s}}\frac{\partial f}{\partial \ell_s} + \frac{N_0 + \iota_s M_0}{\sqrt{g_s}}\frac{\partial f}{\partial \theta_s}\right) + \frac{\partial}{\partial \varphi_s}\left(\frac{\ell_\theta^2}{\sqrt{g_s}}\frac{\partial f}{\partial \ell_s}\right) - \left[\frac{M_0}{\sqrt{g_s}}, f\right], \tag{5.4}$$

$$A_{22} f = \frac{\partial}{\partial \theta_s}\left(\frac{N_0}{\sqrt{g_s}} f\right) - \frac{\partial}{\partial \varphi_s}\left(\frac{M_0}{\sqrt{g_s}} f\right), \tag{5.5}$$

https://doi.org/10.1017/S0022377815000264 Published online by Cambridge University Press

$$S_1 = 4\pi p_s' \sqrt{g_s} + \frac{\delta N_0 + \iota_s \delta M_0}{\chi_1 \sqrt{g_s}} - \frac{\partial}{\partial \ell_s}\left(\frac{[R_s, Z_s]}{\ell_\theta \chi_1 \sqrt{g_s}}\right), \tag{5.6}$$

$$S_2 = \frac{\partial}{\partial \varphi_s}\left(\frac{\delta M_0}{\chi_1 \sqrt{g_s}}\right) - \frac{\partial}{\partial \theta_s}\left(\frac{\delta N_0}{\chi_1 \sqrt{g_s}}\right). \tag{5.7}$$

In these equations we have defined the Poisson bracket

$$[f, g] \doteq \frac{\partial f}{\partial \theta_s}\frac{\partial g}{\partial \varphi_s} - \frac{\partial f}{\partial \varphi_s}\frac{\partial g}{\partial \theta_s}, \tag{5.8}$$

and the functions

$$\delta M_0 = \frac{\ell_\theta^2}{r_\varphi} + P_\theta + \iota_s \frac{2\ell_\theta^2}{r_\theta} + \chi_1 \iota_s \ell_\theta^2 - M_0 \eta, \tag{5.9}$$

$$\delta N_0 = 2R_s \cos u + \iota_s \frac{\ell_\theta^2}{r_\varphi} + 2P_\varphi + P_\theta + \chi_1 \iota_s' g_{\theta\varphi,s} - N_0 \eta, \tag{5.10}$$

$$\eta = \frac{1}{r_\theta} + \frac{\cos u}{R_s}, \tag{5.11}$$

where $p_s' \doteq dp/d\chi\,|_{\chi=\chi_s}$ and $\iota_s' \doteq d\iota/d\chi\,|_{\chi=\chi_s}$.

5.2. *Numerical method for solution*

We can solve the linear system of differential equations, (5.1), numerically by converting it to a matrix system for the spectral expansion coefficients; that is

$$\delta\theta = \sum_{p=0}^{N-1} \delta\theta_p \mathscr{F}_p, \tag{5.12}$$

$$\delta\chi = \sum_{p=0}^{N-1} \delta\chi_p \mathscr{F}_p. \tag{5.13}$$

Using this approach ensures the accuracy of the linear solver matches that of the nonlinear rootfinder for the zeroth-order equilibrium. We are left with the corresponding block matrix system

$$\begin{bmatrix} A_{11}^{pp'} & A_{12}^{pp'} \\ A_{21}^{pp'} & A_{22}^{pp'} \end{bmatrix} \begin{bmatrix} \delta\theta_{p'} \\ \delta\chi_{p'} \end{bmatrix} = \begin{bmatrix} S_1^p \\ S_2^p \end{bmatrix}. \tag{5.14}$$

The blocks are

$$A_{11}^{pp'} = \int_0^{2\pi} d\theta \int_0^{2\pi} d\varphi\, \mathscr{F}_p \left(\frac{M_0}{\sqrt{g_s}}\frac{\partial \mathscr{F}_{p'}}{\partial \varphi} - \frac{N_0}{\sqrt{g_s}}\frac{\partial \mathscr{F}_{p'}}{\partial \theta}\right), \tag{5.15}$$

$$A_{12}^{pp'} = -\int_0^{2\pi} d\theta \int_0^{2\pi} d\varphi \left(\frac{N_0 + \iota_s M_0}{\sqrt{g_s}}\right) \mathscr{F}_p \mathscr{F}_{p'}, \tag{5.16}$$

$$A_{21}^{pp'} = \int_0^{2\pi} d\theta \int_0^{2\pi} d\varphi \left\{ \left(\frac{2M_0 - \iota_s \ell_\theta^2}{\sqrt{g_s}}\right) \frac{\partial \mathscr{F}_p}{\partial \theta_s}\frac{\partial \mathscr{F}_{p'}}{\partial \ell_s}, \right. \tag{5.17}$$

$$\left. - \left(\frac{N_0 + \iota_s M_0}{\sqrt{g_s}}\right) \frac{\partial \mathscr{F}_p}{\partial \theta_s}\frac{\partial \mathscr{F}_{p'}}{\partial \theta_s} - \frac{\ell_\theta^2}{\sqrt{g_s}}\frac{\partial \mathscr{F}_p}{\partial \varphi_s}\frac{\partial \mathscr{F}_{p_s'}}{\partial \ell_s} - \frac{M_0}{\sqrt{g_s}}\left[\mathscr{F}_p, \mathscr{F}_{p'}\right] \right\}, \tag{5.18}$$

https://doi.org/10.1017/S0022377815000264 Published online by Cambridge University Press

$$A_{22}^{pp'} = A_{11}^{p'p} \tag{5.19}$$

$$S_1^p = \int_0^{2\pi} d\theta \int_0^{2\pi} d\varphi \left\{ \left(4\pi p' \sqrt{g_s} + \frac{\delta N_0 + \iota_s \delta M_0}{\chi_1 \sqrt{g_s}} \right) \mathscr{F}_p - \frac{\partial \mathscr{F}_p}{\partial \ell_s} \left(\frac{[R_s, Z_s]}{\ell_\theta \chi_1 \sqrt{g_s}} \right) \right\}, \tag{5.20}$$

$$S_2^p = \int_0^{2\pi} d\theta \int_0^{2\pi} d\varphi \left[\frac{\partial \mathscr{F}_p}{\partial \theta_s} \left(\frac{\delta N_0}{\chi_1 \sqrt{g_s}} \right) - \frac{\partial \mathscr{F}_p}{\partial \varphi_s} \left(\frac{\delta M_0}{\chi_1 \sqrt{g_s}} \right) \right]. \tag{5.21}$$

The discrete form of the helical derivative $\partial_\ell = \partial_\varphi + \iota_s \partial_\theta$ will vanish if the condition $n \pm \iota m = 0$, or equivalently $nq_s \pm m = 0$. If this occurs for some pair (m, n), then the block matrix in (5.14) will be singular. Because the local equilibrium method treats only a single surface at a time, one can simply avoid regions for which q is close to a low-order rational. This ensures the matrix problem is non-singular. Alternatively, in the case of high-order rational surfaces (for example $q = 21/20$) one can limit the spectral element basis so that the singularity is associated with higher harmonics than those retained in the numerical solution.

5.3. *Numerical check in the axisymmetric limit*

To verify the calculation of radial force balance, we can compare the solution of (5.1) with the standard Miller formulation (Candy et al. 2009). We note that the poloidal flux expansion coefficients ψ_1 and ψ_2 given by (64) and (65) in Candy et al. (2009) are related to χ_1 and χ_2 according to

$$\chi_1 = \psi_1/\iota_s \quad \text{and} \quad \delta\chi = 2\,\frac{\chi_2}{\chi_1^2} = 2\iota_s \frac{\psi_2}{\psi_1^2} + \frac{s}{r_s^2}, \tag{5.22}$$

where $s = (r/q)dq/dr$ is the magnetic shear. In Fig. 2 we compare the spectral solution, (5.14), with the finite-difference solver reported in Candy et al. (2009). This plot verifies the correctness as well as the convergence of the present method in the axisymmetric limit.

6. Expressions for differential operators

For numerical evaluation of certain operators that appear in kinetic theory (for example, the curvature drift or gyroaverage), it is necessary to express the differential forms below in terms of the metric elements on the surface ($g_{\varphi\varphi,s}$, etc) as well as the solutions of the force balance equation ($\delta\theta$). To wit

$$\mathbf{B} \cdot \nabla\theta \Big|_s = \frac{\iota_s}{\sqrt{g_s}}, \tag{6.1}$$

$$\mathbf{B} \cdot \nabla\varphi \Big|_s = \frac{1}{\sqrt{g_s}}, \tag{6.2}$$

$$\mathbf{B} \times \nabla B \cdot \nabla\chi \Big|_s = \frac{1}{g_s} \left[-\frac{\partial B_s}{\partial \theta_s} \left(g_{\varphi\varphi,s} + \iota_s g_{\theta\varphi,s} \right) + \frac{\partial B_s}{\partial \varphi_s} \left(g_{\theta\varphi,s} + \iota_s g_{\theta\theta,s} \right) \right], \tag{6.3}$$

$$\mathbf{B} \times \nabla B \cdot \nabla\theta \Big|_s = \frac{1}{g_s} \left[\left(\frac{B_1}{\chi_1} - \delta\theta \frac{\partial B_s}{\partial \theta_s} \right) \left(g_{\varphi\varphi,s} + \iota_s g_{\theta\varphi,s} \right) - \frac{\partial B_s}{\partial \varphi_s} \left(g_{\chi\varphi,s} + \iota_s g_{\chi\theta,s} \right) \right], \tag{6.4}$$

https://doi.org/10.1017/S0022377815000264 Published online by Cambridge University Press

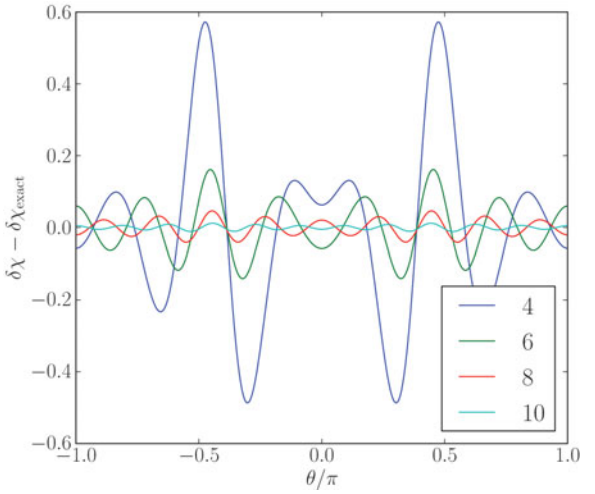


FIGURE 2. Accuracy check of the present spectral solver against an independent implementation of the Miller 2D equilibrium solver. The Miller solver with 1001 gridpoints in θ was used to generate $\delta\chi_{\text{exact}}$. The plot shows rapid convergence as of the spectral solver for $N_\theta = 4, 6, 8, 10$.

$$\mathbf{B}\times\nabla B\cdot\nabla\varphi\Big|_s = \frac{1}{g_s}\left[-\left(\frac{B_1}{\chi_1}-\delta\theta\frac{\partial B_s}{\partial\theta_s}\right)\left(g_{\theta\varphi,s}+\iota_s g_{\theta\theta,s}\right) + \frac{\partial B_s}{\partial\theta_s}\left(g_{\chi\varphi,s}+\iota_s g_{\chi\theta,s}\right)\right], \tag{6.5}$$

where B_1 is defined by the ρ expansion of B; namely

$$B \sim B_s + \rho B_1(\theta_s,\varphi_s) + \mathcal{O}(\rho^2). \tag{6.6}$$

Some algebra shows that

$$\frac{B_1}{B_s} = \frac{\chi_1}{2}\frac{D_0}{N_0+\iota_s M_0}\left(\frac{\iota_s' M_0}{D_0}+\frac{\delta N_0+\iota_s\delta M_0}{\chi_1 D_0}-\frac{D_1}{2D_0}\right). \tag{6.7}$$

An example numerical solution of (4.13) and (5.14) for a 3D local equilibrium is shown in Fig. 3, along with a contour plot of the resulting magnetic field strength B_s.

7. Summary

In the preceding sections, we have developed all the machinery necessary to evaluate first-order differential operators in the neighborhood of a reference three-dimensional flux surface using a local equilibrium method. This method is a generalization of the very popular Miller approach in two dimensions. Below we summarize the basic steps required to complete this procedure:

(*a*) Choose forms for (R_p, Z_p) valid on (and in the neighborhood of) a reference flux surface.

(*b*) Evaluate (R_s, Z_s, J_s) on the reference surface as described in Sec. 3.2, then discard the parameterization (R_p, Z_p).

(*c*) Solve (4.13) for the coefficients $(\alpha_1, \ldots, \alpha_N)$ to obtain $\bar{\theta}(\theta_s)$.

(*d*) Solve (5.14) for the coefficients $(\delta\theta_p, \delta\chi_p)$.

https://doi.org/10.1017/S0022377815000264 Published online by Cambridge University Press

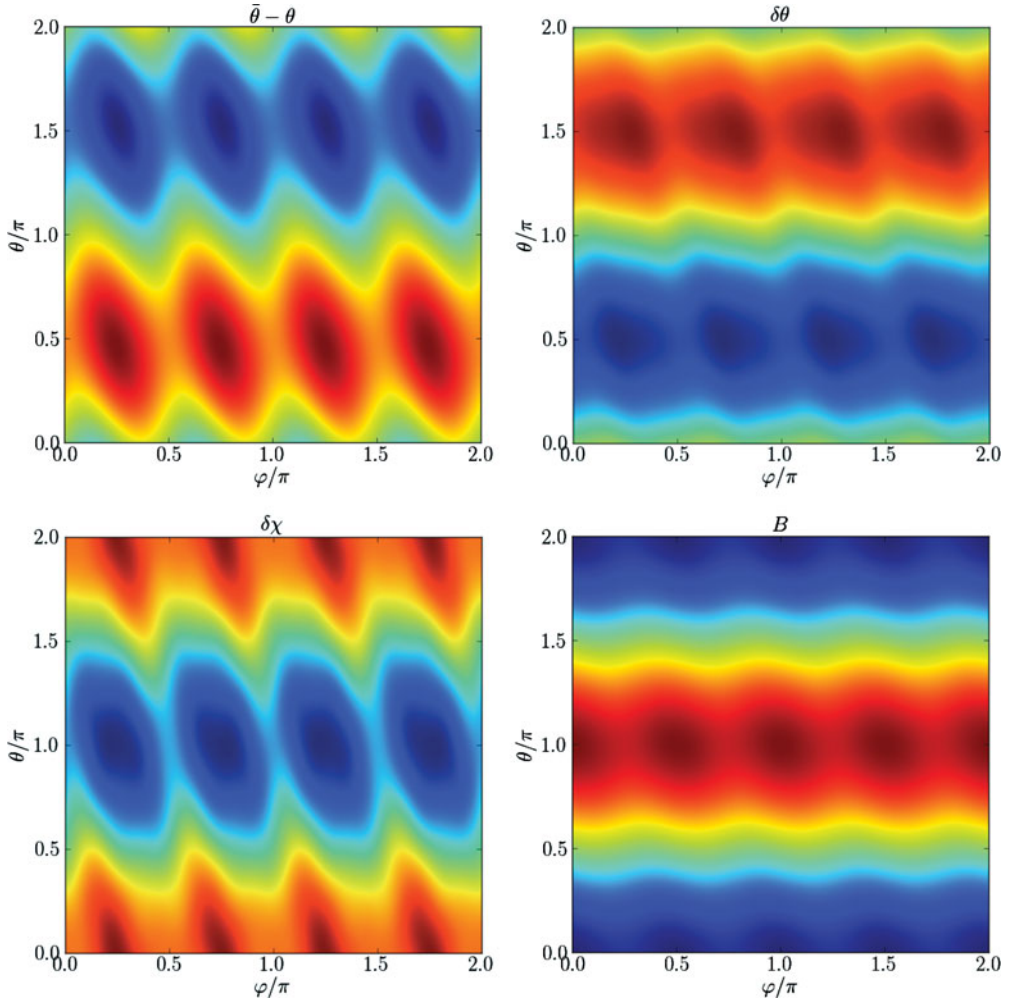


FIGURE 3. Contour maps of $\bar{\theta} - \theta$, $\delta\theta$, $\delta\chi$, and the resulting magnetic field B on the surface for flux-surface shape $R_p = R_0(r) + r\cos\theta + \delta(r)\cos(2\bar{\theta} - 4\bar{\varphi})$, $Z_p = r\sin\bar{\theta} + \delta(r)\sin(2\bar{\theta} - 4\bar{\varphi})$ on the surface $r = r_s = 0.5\,a$. Here, $R_0(r) = 3\,a$, $\delta(r) = 0.015\,a$, $q_s = 2.11$ and $s = 1$.

(*e*) Use the quantities computed in the previous steps to evaluate, for example, the differential operators described in Sec. 6.

Acknowledgements

This material is based upon work supported by the U.S. Department of Energy, Office of Science, Office of Fusion Energy Sciences, Theory program, under Award DE-FG02-95ER54309 and by the Edge Simulation Laboratory project under Grant DE-FC02-06ER54873.

Appendix A. Transformation to Boozer coordinates

The magnetic field, when written in Boozer coordinates $(\chi, \theta_B, \varphi_B)$, takes the form

$$\boldsymbol{B} = B_\theta(\chi)\nabla\theta_B + B_\varphi(\chi)\nabla\varphi_B + B_\chi(\chi, \theta_B, \varphi_B)\nabla\chi. \tag{A 1}$$

https://doi.org/10.1017/S0022377815000264 Published online by Cambridge University Press

Dotting the above (contravariant) form of $\boldsymbol{B}$ with the covariant form gives the familiar result $B^2 = (\iota I + J)/\sqrt{g_B}$, where $\sqrt{g_B}$ is the Boozer Jacobian. Since the Boozer angles are themselves straight fieldline angles, they can be related to the straight fieldline angles of the present work according to

$$\theta = \theta_B + \iota\omega(\chi, \theta_B, \varphi_B), \tag{A 2}$$

$$\varphi = \varphi_B + \omega(\chi, \theta_B, \varphi_B), \tag{A 3}$$

where ω is a doubly-periodic generating function. Relating (A 1) and (2.1), we find that the equations determining ω are

$$\boldsymbol{B}\cdot\frac{\partial \boldsymbol{x}}{\partial\theta} = \frac{1}{\sqrt{g}}\left(g_{\theta\varphi} + \iota g_{\theta\theta}\right) = B_\theta - \frac{\partial\omega}{\partial\theta}(B_\varphi + \iota B_\theta), \tag{A 4}$$

$$\boldsymbol{B}\cdot\frac{\partial \boldsymbol{x}}{\partial\varphi} = \frac{1}{\sqrt{g}}\left(g_{\varphi\varphi} + \iota g_{\theta\varphi}\right) = B_\varphi - \frac{\partial\omega}{\partial\varphi}(B_\varphi + \iota B_\theta), \tag{A 5}$$

$$\boldsymbol{B}\cdot\frac{\partial \boldsymbol{x}}{\partial\chi} = \frac{1}{\sqrt{g}}\left(g_{\chi\varphi} + \iota g_{\chi\theta}\right) = B_\chi - \frac{\partial\omega}{\partial\chi}(B_\varphi + \iota B_\theta). \tag{A 6}$$

The first two equations show that the condition for zero radial current, (2.14), is satisfied by arbitrary B_θ and B_φ. From these relations, we see at once that the flux functions in (A 3) can be expressed as the integrals

$$B_\theta(\chi) = \frac{1}{2\pi}\int_0^{2\pi} d\theta\, \frac{g_{\theta\varphi} + \iota g_{\theta\theta}}{\sqrt{g}}, \tag{A 7}$$

$$B_\varphi(\chi) = \frac{1}{2\pi}\int_0^{2\pi} d\varphi\, \frac{g_{\varphi\varphi} + \iota g_{\theta\varphi}}{\sqrt{g}}. \tag{A 8}$$

Once these flux-functions are determined, the value of ω on the surface can then be computed via the solution of the first two differential equations. To obtain B_χ and the variation of ω off the surface, the formalism of Sec. 3.2 must be used. Finally, we remark that in the case of an unshifted axisymmetric circle, we find

$$B_{\theta s} = \iota_s r_s^2 B_{\text{unit}}\left\langle\frac{1}{R_s}\right\rangle, \tag{A 9}$$

$$B_{\varphi s} = B_{\text{unit}}\left\langle\frac{1}{R_s}\right\rangle^{-1}, \tag{A 10}$$

$$\theta_{Bs} = \theta_s, \tag{A 11}$$

$$\varphi_{Bs} = \varphi_s, \tag{A 12}$$

$$\omega_s = 0, \tag{A 13}$$

where the angle brackets denote an average over θ.

REFERENCES

Baumgaertel, J. A., Belli, E. A., Dorland, W., Guttenfelder, W., Hammett, G. W., Mikkelsen, D. R., Rewoldt, G., Tang, W. M. and Xanthopoulos, P. 2011 Simulating gyrokinetic microinstabilities in stellarator geometry with GS2. *Phys. Plasmas* **18**, 122 301.

Bird, T. M. and Hegna, C. C. 2013 A model for microinstability destabilization and enhanced transport in the presence of shielded 3D magnetic perturbations. *Nucl. Fusion* **53**, 013 004.

Bishop, C. M., Kirby, P., Connor, J. W., Hastie, R. J. and Taylor, J. B. 1984 Ideal MHD ballooning stability in the vicinity of a separatrix. *Nucl. Fusion* **24**, 1579.

https://doi.org/10.1017/S0022377815000264 Published online by Cambridge University Press

Boozer, A. H. 2002 Local equilibrium of nonrotating plasmas. *Phys. Plasmas* **9**, 3762.

Candy, J. 2009 A unified method for operator evaluation in local Grad-Shafranov plasma equilibria. *Plasma Phys. Control. Fusion* **51**, 105 009.

Candy, J., Holland, C., Waltz, R. E., Fahey, M. R. and Belli, E. 2009 Tokamak profile prediction using direct gyrokinetic and neoclassical simulation. *Phys. Plasmas* **16**, 060 704.

Greene, J. M. and Chance, M. S. 1981 *Nucl. Fusion* **21**, 453.

Hegna, C. C. 2000 Local three-dimensional magnetostatic equilibria. *Phys. Plasmas* **7**, 3921.

Hirshman, S. P., Shaing, K. C., van Rij, W. I., C. O. Beasley, Jr. and E. C. Crume, Jr. 1986 Plasma transport coefficients for nonsymmetric toroidal confinement systems. *Phys. Fluids* **29**, 2951.

Hirshman, S. P. and Whitson, J. C. 1983 Steepest-descent moment method for three-dimensional magnetohydrodynamic equilibria. *Phys. Fluids* **26**, 3553.

Landreman, M., Smith, H. M., Mollen, A. and Helander, P. 2014 Comparison of particle trajectories and collision operators for collisional transport in nonaxisymmetric plasmas. *Phys. Plasmas* **21**, 042 503.

Mercier, C. and Luc, N. 1974 *Tech. Rep.* Commission of the European Communities, Report No. EUR-5127e 140, Brussels.

Miller, R. L., Chu, M. S., Greene, J. M., Lin-liu, Y. R. and Waltz, R. E. 1998 Noncircular, finite aspect ratio, local equilibrium model. *Phys. Plasmas* **5**, 973.

Moré, J. J., Garbow, B. S. and Hillstrom, K. E. 1980 User guide for MINPACK-1. *Tech. Rep.* ANL-80-74. Argonne National Laboratory, Argonne, IL, USA.

van Rij, W. I. and Hirshman, S. P. 1989 Variational bounds for transport coefficients in three-dimensional toroidal plasmas. *Phys. Fluids* B **1**, 563.

Waltz, R. E. and Miller, R. L. 1999 Ion temperature gradient turbulence simulations and plasma flux surface shape. *Phys. Plasmas* **6**, 4265.

Xanthopoulos, P., Merz, F., Görler, T. and Jenko, F. 2007 Nonlinear gyrokinetic simulations of Ion-temperature-gradient turbulence for the optimized Wendelstein 7-X stellarator. *Phys. Rev. Lett.* **99**, 035 002.

https://doi.org/10.1017/S0022377815000264 Published online by Cambridge University Press